ICIC Express Letters
Part B: Applications
Volume **7**, Number **11**, November **2016**

ICIC International ©2016 ISSN 2185-2766
pp. **2435–2442**

DEVELOPMENT AND EXPERIMENTAL STUDY OF A NOVEL WEAK COUPLING PARALLEL THREE-DIMENSIONAL FORCE SENSOR

Yanzhi Zhao[1,2], Leihao Jiao[1,2], Dacheng Weng[1,2]
Yang Li[1,2] and Xiaoxiao Liu[1,2]

[1]Key Laboratory of Parallel Robot and Mechatronic System of Hebei Province
[2]Key Laboratory of Advanced Forging and Stamping Technology and Science
of Ministry of Education of China
Yanshan University
No. 438, Hebei Ave., Qinhuangdao 066004, P. R. China
yzzhao@ysu.edu.cn

Received April 2016; accepted July 2016

Abstract. *In order to effectively reduce the effect of coupling, a novel mechanical decoupling parallel three-dimensional force sensor with the steel ball structure is designed and developed, and the static calibration of the sensor is carried out. The rolling friction is applied instead of sliding friction to the design of the mechanical decoupling parallel three-dimensional force sensor. The mathematic model of the sensor is established, and the force mapping relationship of the applied external force and the force of measuring branches of the sensor is derived based on the screw theory. The prototype of the mechanical decoupling parallel three-dimensional force sensor is developed, and the load calibration and data acquisition experiment system are developed, and the static calibration is performed. The calibration data are analyzed by using the least-squares method and the experimental result shows that the interference error is less than 0.45% and the measurement error of the sensor prototype is less than 0.6%, which indicate that the developed mechanical decoupling parallel three-dimensional force sensor possesses high measurement accuracy, and the result of the study lays the foundation of the application of the mechanical decoupling parallel three-dimensional force sensor.*
Keywords: Three-dimensional force sensor, Mechanical decoupling, Parallel mechanism, Static calibration

1. **Introduction.** The multi-dimensional force sensor is one kind of the most important sensors since it has the ability of measuring three force components and three torque components, and it has been applied widely in many research areas, such as robotics, automobile industry, wind tunnel balances and aeronautics [1]. In the development of multi-dimensional force sensor, the coupling problem is an important factor limiting measuring accuracy of a multi-dimensional force sensor. In order to effectively reduce the effect of coupling, a lot of works are carried out on the design of elastic structure and decoupling algorithm by domestic and overseas scholars. Vázsonyi et al. [2] designed a three-dimensional force sensor by novel alkaline etching technique. Beccai et al. [3] designed and developed a silicon-based three-dimensional force sensor to be used in a flexible smart interface for biomechanical measurements. Gao et al. [4] developed a six-dimensional force sensor based on Stewart platform, and introduced the elastic joints to replace the real spherical joints which made the miniaturization possible. Cui et al. [5] proposed and developed a novel three-dimensional force/torque sensor by optimizing the elastic body structure with orthogonal test method. Zhang et al. [6] carried out a study on a new type of adopted structure for three dimensions strain gauge force sensor which can be used for measuring three-dimensional forces Fx, Fz, and My. Liu et al. [7] put

forward a high sensitivity 3D torque sensor, which is to measure 3D torque and solve problem of coupling between two dimensions. Yu et al. [8] carried out a study on design and decoupling test of a miniature three dimensions force sensor with a new elastomer structure. Certain achievements are obtained in the above researches, but the dimensional coupling of the designed sensors based on the traditional parallel structure is relatively serious. So the design of a novel structure will provide an essential supplement and open up a new direction for the research of novel weak coupling multi-dimensional force sensor.

In this paper, a novel mechanical decoupling parallel three-dimensional force sensor with steel ball structure is proposed which is currently in the process of patenting [9], and the mathematical model of the three-dimensional force sensor is established, and then the force mapping relationship of the applied external force and the force of measuring limbs of the sensor is derived based on the screw theory and the rolling friction. Besides, the prototype of the mechanical decoupling parallel three-dimensional force sensor is developed, and the load calibration and the data acquisition experiment system of the sensor are developed, and the static calibration is carried out.

The organization of this paper is as follows. Following the introduction, the structural analysis of the sensors, including the mechanical structure feature of the sensor and the advantages of the proposed sensor with steel ball contact structure, are shown in Section 2. Section 3 concerns the measuring model of the structure, and the force mapping relationship between the applied external force and the force of measuring branches of the sensor is derived. Section 4 introduces the sensor prototype and the experimental study of static calibration of the sensor prototype. The paper is concluded in Section 5, summarizing the present work.

2. **The Structure of the Sensor.**

Figure 1 illustrates the diagram of the mechanical decoupling parallel three-dimensional force sensor with steel ball structure. It mainly consists of a loading plate, a frame, a connecting plate, a base and four force-measuring branches which are divided into two groups, three horizontal force-measuring branches are distributed around the force plate, and the other branch is located just below the force-measuring plate. Each force-measuring branch contains a single-dimensional force sensor, a steel ball and an arc indenter connected with the force-measuring plate using the steel ball.

Due to the application of the steel ball structure, the pre-stressed force is needed to ensure that all the force-measuring branches are always in compression when subjected to the expected range of external loads. The number of the pre-stressed forces is determined

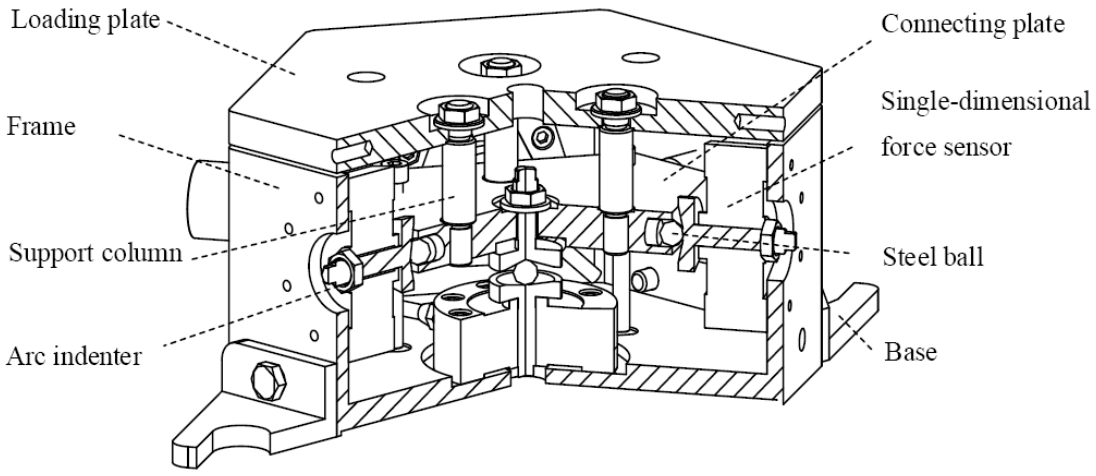

FIGURE 1. Structure diagram of the parallel three-dimensional force sensor

by measuring the range of the designed sensor, and by pre-stressing arc indenter properly, the sensor can bear an anticipant pre-compression force.

The mechanical decoupling parallel three-dimensional force sensor has several advantages over the current designs based on traditional parallel structure with simple structure and high stiffness. Firstly, by replacing the traditional spherical pairs with steel ball contact structure, the friction and frictional moment are greatly reduced. In addition, providing that a sufficient pre-stressing force acts on the sensor, each branch will just sustain compressive force within the measurement range of the sensor. Furthermore, as the sensor is developed by replacing the sliding friction with rolling friction, the mechanical decoupling is realized, and the effect of coupling is reduced significantly.

3. Measurement Model of the Sensor.

According to the designed structure of the mechanical decoupling parallel three-dimensional force sensor, the force-measuring branch is simplified to P-S structure where P denotes the planar pair and S denotes the spherical pair. The force mapping relationship between the applied external force and the force of measuring branches of the sensor is derived based on the screw theory.

3.1. The force mapping relationship in ideal case.

Figure 2 illustrates the simplified diagram of the sensor, and the symbols are defined as follows: a_i and A_i denote the contact points of the branch connected with the connecting plate and the base respectively. f_w and m_w denote the external force and external toque.

The force diagram of the connecting plate is shown in Figure 3. Each branch can only bear the axis force ignoring the gravity of the branch and the friction of joints.

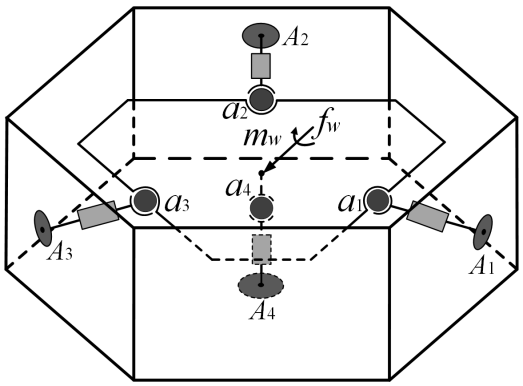

FIGURE 2. Simplified diagram of the sensor

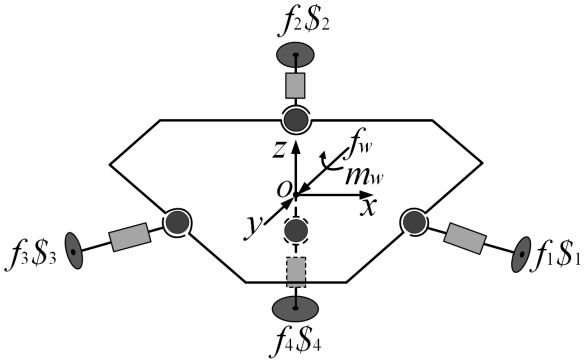

FIGURE 3. Force diagram of the connecting plate

The static equilibrium equation of the connecting plate can be obtained based on the screw theory [9].

$$F_W = \sum_{i=1}^{4} f_i \$_i \tag{1}$$

where $F_W = (f_w \quad m_w)^T$ represents the generalized vector of the external force; f_i represents the reacting force on the ith branch; $\$_i = (S_i \quad S_{0i})$ represents the unit line vector along the ith leg.

Equation (1) can be rewritten in other forms as

$$\left.\begin{aligned} f_w &= \sum_{i=1}^{4} f_i S_i \\ m_w &= \sum_{i=1}^{4} f_i S_{0i} \end{aligned}\right\} \tag{2}$$

where $f_w = (f_{wx} \quad f_{wy} \quad f_{wz})^T$, $m_w = (m_{wx} \quad m_{wy} \quad m_{wz})^T$, $S_i = (a_i - A_i)/|a_i - A_i|$, $S_{0i} = (A_i \times a_i)/|a_i - A_i|$.

Equation (1) can also be rewritten in the form of matrix equation as:

$$F_W = Gf \tag{3}$$

where $f = (f_1 \quad f_2 \quad f_3 \quad f_4)^T$ is the vector composed of the reacting forces of the four branches; G is the static mapping matrix which is given by:

$$G = \begin{bmatrix} S_1 & S_2 & S_3 & S_4 \\ S_{01} & S_{02} & S_{03} & S_{04} \end{bmatrix}_{3\times 4} \tag{4}$$

Combine the structure parameter of the sensor, the static mapping matrix can be derived as:

$$G = \begin{bmatrix} -1 & \sqrt{3}/2 & \sqrt{3}/2 & 0 \\ 0 & -1/2 & 1/2 & 0 \\ 0 & 0 & 0 & -1 \end{bmatrix} \tag{5}$$

3.2. **Force mapping relationship in consideration of the pre-stressed force.** As shown in Figure 4, the pre-stressed force is needed to ensure that all the force-measuring branches are always in compression when subjected to the expected range of external loads. Under the action of the pre-stressed force, the friction will be produced which can affect the coupling. So the force mapping relationship is derived in consideration of the pre-stressed force.

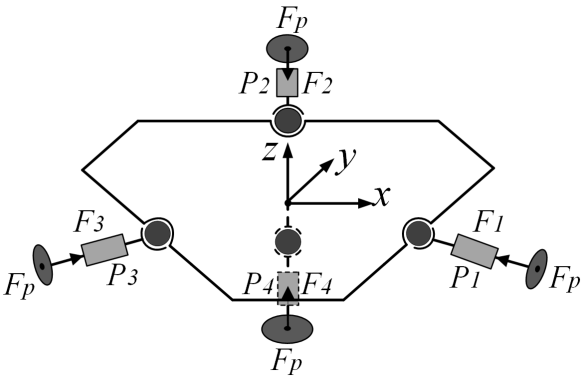

FIGURE 4. The diagram of pre-stressed force acting on the branches

In Figure 4, F_p represents the pre-stressed force acting on the branches, P_i $(i = 1, 2, 3, 4)$ represents the loading direction of the pre-stressed force. F_i $(i = 1, 2, 3, 4)$ represents the values of the force-measuring branches.

So according to Figure 4, the static equilibrium equation of the connecting plate can be established as:

$$\left.\begin{aligned} F_x - (F_1 + F_p) - (F_2 + F_p)\cos\theta - (F_3 + F_p)\cos\theta - f_2'\cos 30^\circ - f_3'\cos 30^\circ - 3f_4' = 0 \\ F_y - (F_2 + F_p)\sin\theta - (F_3 + F_p)\sin\theta - f_1' - f_2'\cos 30^\circ - f_3'\cos 30^\circ - 3f_4' = 0 \\ F_z - (F_4 + F_p) - f_1' - f_2' - f_3' = 0 \end{aligned}\right\} \tag{6}$$

where θ represents the half angle between horizontal branches; f_i' represents the horizontal thrust when the steel ball is in a critical rolling state, which can be obtained based on the rolling friction theory [10].

$$f_i' = \delta\,(F_i + F_p)/R \tag{7}$$

where δ represents the coefficient of rolling friction which is determined by the material, and in this paper, the coefficient of rolling friction of the steel ball is 0.01; R represents

the steel ball radius which is 12mm in this paper. So Equation (6) can be simplified as:

$$\begin{bmatrix} F_x \\ F_y \\ F_z \end{bmatrix} = G' \begin{bmatrix} F_1 + F_p \\ F_2 + F_p \\ F_3 + F_p \\ F_4 + F_p \end{bmatrix} = \begin{bmatrix} 1 & -1.22 & -1.22 & -0.83 \\ -0.83 & 0.45 & -1.29 & -0.83 \\ -0.83 & -0.83 & -0.83 & 1 \end{bmatrix} \begin{bmatrix} F_1 + F_p \\ F_2 + F_p \\ F_3 + F_p \\ F_4 + F_p \end{bmatrix} \tag{8}$$

where G' represents the static mapping matrix in consideration of the pre-stressed force, which can be obtained as:

$$G' = \begin{bmatrix} 1 & -1.22 & -1.22 & -0.83 \\ -0.83 & 0.45 & -1.29 & -0.83 \\ -0.83 & -0.83 & -0.83 & 1 \end{bmatrix} \tag{9}$$

4. Static Calibration of the Sensor.

4.1. **The prototype of the sensor.** In order to prove the superiority of the proposed sensor structure and prove the correctness of the theoretical analysis, a mechanical decoupling parallel three-dimensional force sensor is manufactured, and the static calibration experiment is carried out. The design diagram and the object are shown in Figure 5. Each leg of the sensor contains a single-dimensional force sensor used for measuring the reacting force. To ensure adequate stiffness and light weight, the frame and the connecting plate are machined from steel ingot. The material of the arc indenter is 42CrMo, and in order to reduce the measuring error caused by the deformation of the arc indenter, a heat-treatment is needed. The expected maximal external force is ±3000N.

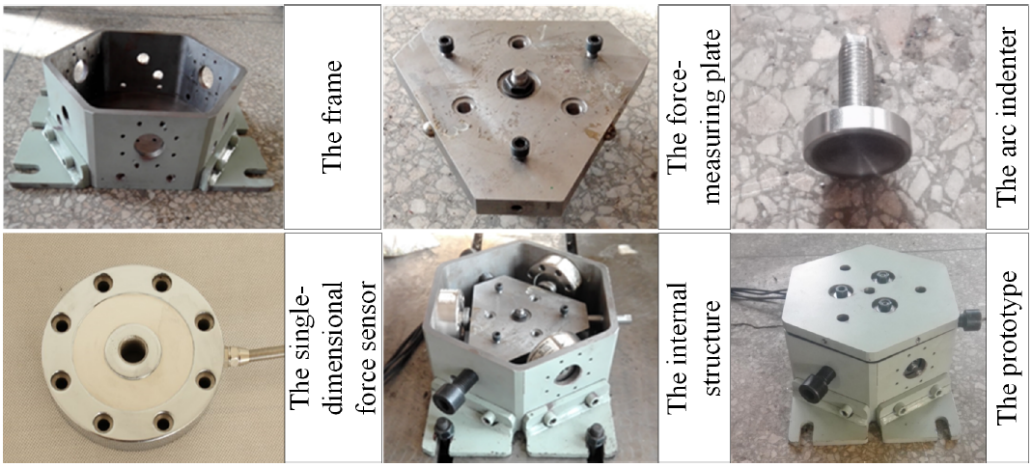

FIGURE 5. The prototype of the sensor

4.2. **The static calibration.** In order to prove the mechanical decoupling effect of the sensor with steel ball, a special calibration device is designed, and the static calibration is carried out. The load calibration and data acquisition experiment system are developed, and the device mainly consists of standard single-dimensional force sensor, prototype of the developed sensor, intelligent instrument and computer. Figure 6 illustrates the schematic diagram of the calibration experiment, and Figure 7 illustrates the loading experiment.

The full scale of the sensor is divided into 10 points, and each load orientation contains load and offload procedures with 300N step length. The relationship between the measured value and the loading force can be established as:

$$F_s = GF + Err \tag{10}$$

where F_s represents the loading force, G is the static mapping matrix, F represents the measured value of each sensor, and Err represents the error matrix which is defined as:

$$Err = (F_s - F)/F_{\max} \tag{11}$$

where $F_{\max}$ represents the full scale of the sensor.

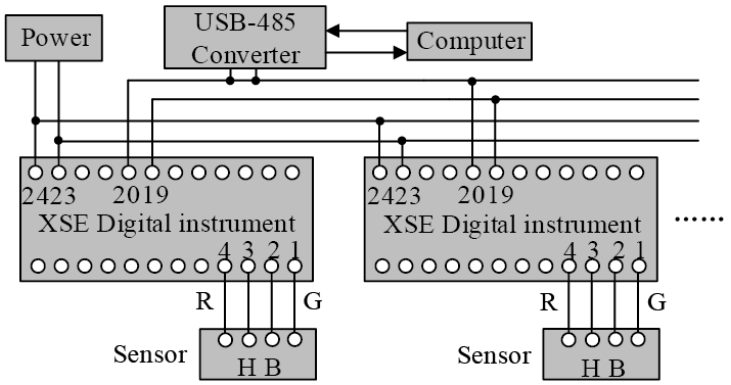

FIGURE 6. Schematic diagram of the calibration

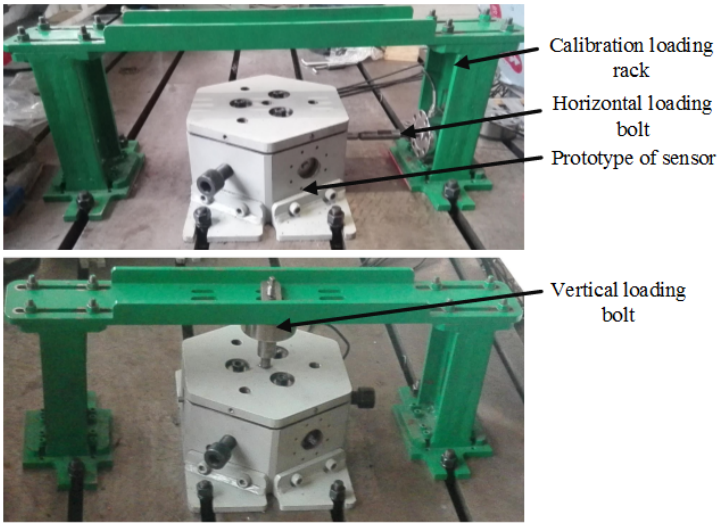

FIGURE 7. The static calibration experiment

According to the least square theory, the following relationship can be obtained:

$$\frac{\partial J_i}{\partial G_i}\Big|_{G_i=\overline{G_i}} = \frac{\partial \left(F_s i - F^T G_i\right)^T \left(F_s i - F^T G_i\right)^T}{\partial G_i}\Big|_{G_i=\overline{G_i}} = 0 \tag{12}$$

where G_i represents the ith dimension of the mapping matrix, and $\overline{G}_i$ represents the ith dimension of the augmented mapping matrix.

According to Equation (12) and the structure of the sensor, the mapping matrix is obtained as:

$$G = \left[\begin{array}{cccc} \overline{G_1} & \overline{G_2} & \overline{G_3} & \overline{G_4} \end{array}\right] = F_s F^T \left(F F^T\right)^{-1} \tag{13}$$

In this paper, the static calibration experiment is carried out when the pre-stressed force is 700N, and the calibration data is acquired. The mapping matrix can be obtained combining the calibration data based on the least square theory.

$$G = \left[\begin{array}{cccc} 0.9889 & -0.5209 & -0.5357 & -0.0077 \\ -0.0048 & 0.8656 & -0.8849 & 0.0252 \\ -0.0294 & 0.0085 & -0.0922 & -1.0387 \end{array}\right] \tag{14}$$

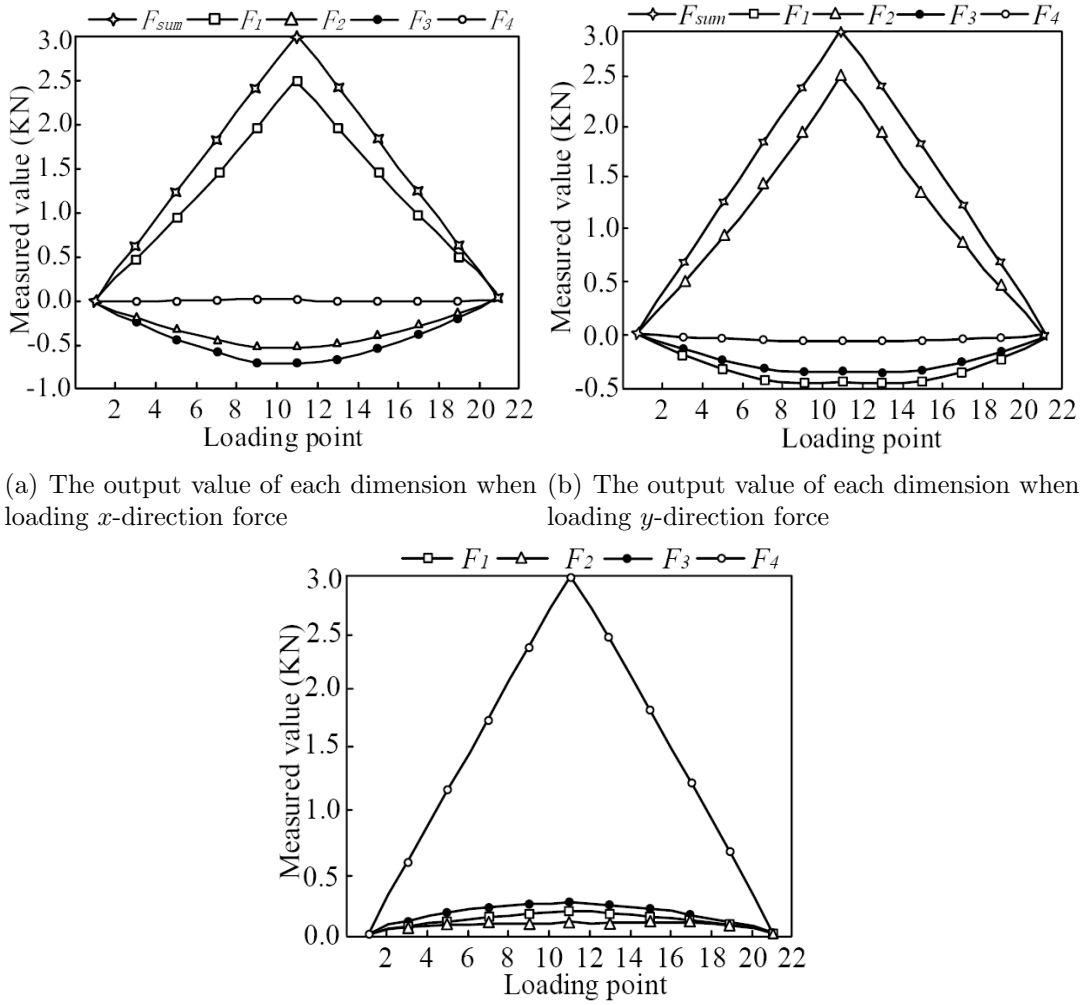

(a) The output value of each dimension when loading x-direction force

(b) The output value of each dimension when loading y-direction force

(c) The output value of each dimension when loading z-direction force

FIGURE 8. The output value of each dimension in the static calibration

The relationship between the measured value of each branch and the synthetic force obtained through projecting the loading force to the coordinate axes and the corresponding diagram are presented in Figure 8.

The measuring error along x axis can be expressed as based on the defined error matrix in Equation (11).

$$E_x = \begin{pmatrix} \max(\Delta F_{x1})/F_{xm} & \max(\Delta F_{x2})/F_{ym} & \max(\Delta F_{x3})/F_{zm} \end{pmatrix}^T \tag{15}$$

where E_x represents the measuring error along x axis, F_{im} $(i = x, y, z)$ represents the full scale along i axis, and ΔF_{xi} $(i = 1, 2, 3)$ represents the maximum error in the ith calibration.

The means applies equally to y axis and z axis, so the measuring error matrix of the sensor can be expressed as:

$$Err = \begin{pmatrix} E_x & E_y & E_z \end{pmatrix} \tag{16}$$

The measurement error matrix can be obtained combining the calibration data as shown in Equation (17):

$$Err = \begin{bmatrix} 0.0037 & 0.0013 & 0.0028 \\ 0.0025 & 0.0017 & 0.0027 \\ 0.0041 & 0.0045 & 0.0060 \end{bmatrix} \tag{17}$$

The measurement error matrix shows that the coupling error is less than 0.45%. The static calibration results show that measurement error of the designed mechanical decoupling parallel three-dimensional force sensor is less than 0.6%, and the results prove that the sensor can be used in the industrial production with high measurement requirements.

5. Conclusions.

(1) A novel mechanical decoupling parallel three-dimensional force sensor is proposed and manufactured, which possesses not only the advantages of traditional parallel structure but also the performance of mechanical decoupling.
(2) The mathematic model of the sensor is established, and the force mapping relationship between the applied external force and the force of measuring branches of the sensor is derived based on the screw theory and the rolling friction theory.
(3) The load calibration and data acquisition experiment system of the sensor are developed, and the static calibration is carried out with the least square calibration method, and the results show that the coupling error is less than 0.45% and the measurement error is less than 0.6%.
(4) In the near future, further optimization of the sensor will be paid attention to. The aim is that the proposed sensor can be mostly used in the large range spacial three dimensional force measurement in the industrial production.

Acknowledgment. The research work is supported by the National Natural Science Foundation of China (Grant No. 51105322), and Hebei Provincial Natural Science Foundation of China (Grant No. E2014203176), Hebei Provincial Natural Science Research Project for Distinguished Young Scholars in Higher Education Institution (No. QN20150 40) and China's Post-doctoral Science Fund (No. 2016M590212).

REFERENCES

[1] C. Mao, A. G. Song, X. Gao et al., Research and application of static decoupling algorithm for six-axis force/torque sensor, *Chinese Journal of Sensors and Actuators*, vol.28, no.2, pp.205-210, 2015.
[2] É. Vázsonyi, M. Adam, C. Dücsõ et al., Three-dimensional force sensor by novel alkaline etching technique, *Sensors and Actuators A*, vol.123, pp.620-626, 2005.
[3] L. Beccai, S. Roccella et al., Design and fabrication of a hybrid silicon three-axial force sensor for biomechanical applications, *Sensors and Actuators A*, vol.120, pp.620-626, 2015.
[4] F. Gao, Z. L. Jin et al., Development of a new type of 6-DOF parallel micro-manipulator and its control system, *Proc. of IEEE Int. Conf. Robot. Intell. Syst. Signal Process*, Changsha, China, pp.715-720, 2003.
[5] Y. Cui, S. X. Zhang and Z. Cui, Development of a novel three-dimensional force/torque sensor, *Machinery Manufacturing*, vol.53, no.609, pp.25-28, 2015.
[6] H. X. Zhang, J. W. Cui and D. F. Chen, Study on a new type of adopted structure for three dimensions strain gauge force sensor, *Chinese Journal of Sensors and Actuators*, vol.27, no.2, pp.162-167, 2014.
[7] X. D. Liu, X. W. Gu, J. Ban et al., Design and calibration of high sensitivity 3D torque sensor, *Transducer and Microsystem Technologies*, vol.33, no.8, pp.76-79, 2014.
[8] Z. W. Yu, J. Gong, Q. Wu et al., Study on design and decoupling test of a miniature three dimensions force sensor, *Chinese Journal of Sensors and Actuators*, vol.25, no.1, pp.38-43, 2012.
[9] Y. Z. Zhao, D. C. Weng et al., A novel tension compression bidirectional decoupling parallel three-dimensional force sensor, *Chinese Patent: 201410451751.5*, 2014.
[10] Z. Huang, Y. S. Zhao and T. S. Zhao, *Advanced Spatial Mechanism*, Higher Education Press, Beijing, China, 2006.
[11] Harbin Institute of Technology, *Theoretical Mechanics*, Higher Education Press, Beijing, China, 2002.